Photon Spectrum from Radiative μ Capture in Calcium*

L. M. Rosenstein† and I. S. Hammerman
Columbia University, New York, New York 10027
(Received 8 August 1972; revised manuscript received 20 April 1973)

We have measured the high-energy end of the γ-ray spectrum from radiative muon capture in calcium. This accounted for only about one half of the neutral events detected beyond 57 MeV, the rest apparently being due to neutrons emitted by nuclei after capture. By fitting a theoretical prediction of the photon spectrum to our data, we found a value for the induced pseudoscalar coupling constant which disagrees with that expected.

The internal bremsstrahlung of radiative muon capture in calcium comes from the basic process

$$\mu^- + p \rightarrow n + \nu_\mu + \gamma$$

occurring inside the ^{40}Ca nucleus. We here report the results of an experiment which measured the upper end of the energy spectrum of these photons. A previous article[1] presented our analysis of the angular distribution of these γ rays with respect to the muon spin polarization.

In the experiment, a negative beam from the Nevis synchrocyclotron passed through a copper moderator which removed pions and slowed the muons so they stopped in a 5.9-g/cm^2-thick calcium target, placed at 45° with respect to the beam. The stopping of a muon in the target, or μ stop, was defined by coincident signals from four beam counters in anticoincidence with a fifth, C-shaped counter, surrounding the target on three sides. Typically, we recorded 5000 μ stops/sec and our results are based on a total of 1.2×10^{10} μ stops.

In order to detect γ rays and electrons (from the ordinary decay of bound muons, which competes with the capture process) leaving the calcium at all angles with respect to the muon polarization, the target was placed between the poles of a dipole magnet having an average field of 446 G in the capture region. This caused the muon spin to precess with a period of 165 nsec (about one half the bound-muon lifetime) and thus allowed a stationary detector to view all directions with respect to the muon spin as a function of time.

The detector itself was a 23.8-cm-diam by 25.4-cm-deep cylindrical NaI(Tl) crystal placed with its axis perpendicular to the initial beam line (see Fig. 1 in Ref. 1). Three large veto counters covered the crystal on two sides and on top, and a fourth one, V_4, covered its front face. A 15.24-cm-diam hole in the lead shielding surrounding the veto counters and crystal collimated particles from the target so none would have too short a path length in the crystal for accurate energy measurement. A photon signal in the NaI crystal, or γ-out event, was denoted by a pulse from the NaI, above a 40-MeV threshold, in anticoincidence with all of the veto counters and the first beam counter (counter 1). An electron event, or e out, was defined by a coincidence among two 15.24-cm counters placed at either end of the lead collimator and V_4, and an anticoincidence with counter 1.

We calibrated our crystal for the energy measurement of photons (and electrons) by replacing the calcium target by a similarly shaped block of LiH and recording the spectrum of γ rays emitted when π^-'s were stopped in the new target. After a short run, this process was repeated with a Li target and the resulting photon energy spectrum of the latter was subtracted from that of the former. The resulting distribution is shown in Fig. 1 and represents the capture of negative pions by hydrogen (i.e., protons) in the reactions

$$\pi^- + p \rightarrow n + \gamma,$$

$$\pi^- + p \rightarrow n + \pi^0 \searrow \gamma + \gamma.$$

The photon from the first reaction has a unique energy of 129.4 MeV and therefore it also provided the resolution function of the crystal.[2] This was checked by folding the resolution function (15.6% full width at half maximum) thus derived into the theoretical, flat distribution of photons from the second reaction above, and we did in fact reproduce the low-energy bump in Fig. 1, peaking at 60.5 MeV.

The time between the occurrence of μ-stop and γ-out signals was also measured.[1] This was done by having each γ-out event produce a 700-nsec-wide electronic gate that was sent to two coincidence modules. A μ-stop event initiated two short pulses, one delayed approximately the length of a gate, each going to one of the coincidence units. If the direct pulse produced a coincidence with the γ-out gate, it must have occurred after the γ-out event in real time, and therefore the

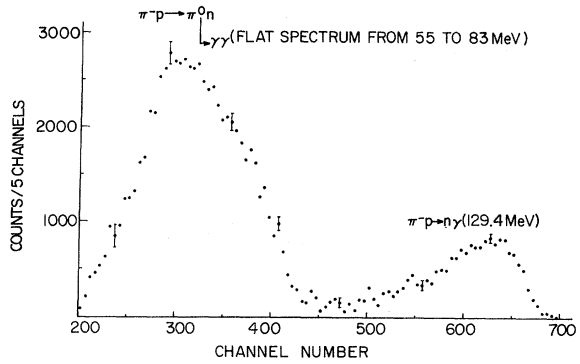

FIG. 1. Energy spectrum of "LiH-Li."

latter must have been due to a (μ-stop-independent) background event (see discussion of background that follows), which we labeled B_γ. As shown in Ref. 1, the time distribution of these μ-stop-independent events was found, indeed, to be time-independent. A coincidence with the delayed pulse, on the other hand, required that the μ stop precede the γ out in real time and was designated a foreground event, F_γ. A similar timing system was used for electrons, with coincidences labeled B_e and F_e.[3]

Due to the slow rate of true radiative muon captures, the potentially large background represented a serious problem. NaI signals due to charged-particle background were essentially eliminated by the lead shielding and veto counters surrounding the crystal. The neutral background radiation may be divided into two classes: time-independent and time-dependent. Background not directly associated with a μ stop will produce a uniform time distribution of NaI pulses and is therefore given by the B_γ events mentioned earlier. If the B_γ energy spectrum is then subtracted from that for F_γ, we are left only with foreground events which are associated with μ stops. The B_γ and F_γ spectra are shown in Fig. 2(a).

Time-dependent background, correlated with μ stops, was more troublesome. The largest γ-ray contamination came from bremsstrahlung in the calcium target given off by electrons from muon decay. This could not be distinguished from capture γ rays, so we were forced to look only at photons above the 53-MeV kinematical energy limit of the bremsstrahlung. (Actually, we used 57 MeV as a lower limit for reasons explained in Ref. 1.) The contamination from bremsstrahlung in any of our data points above this energy is negligible. Another source of contamination was muons captured by carbon atoms present in the scintillation counters and wrapping material. However, it was shown in Ref. 1 that electrons from decay of

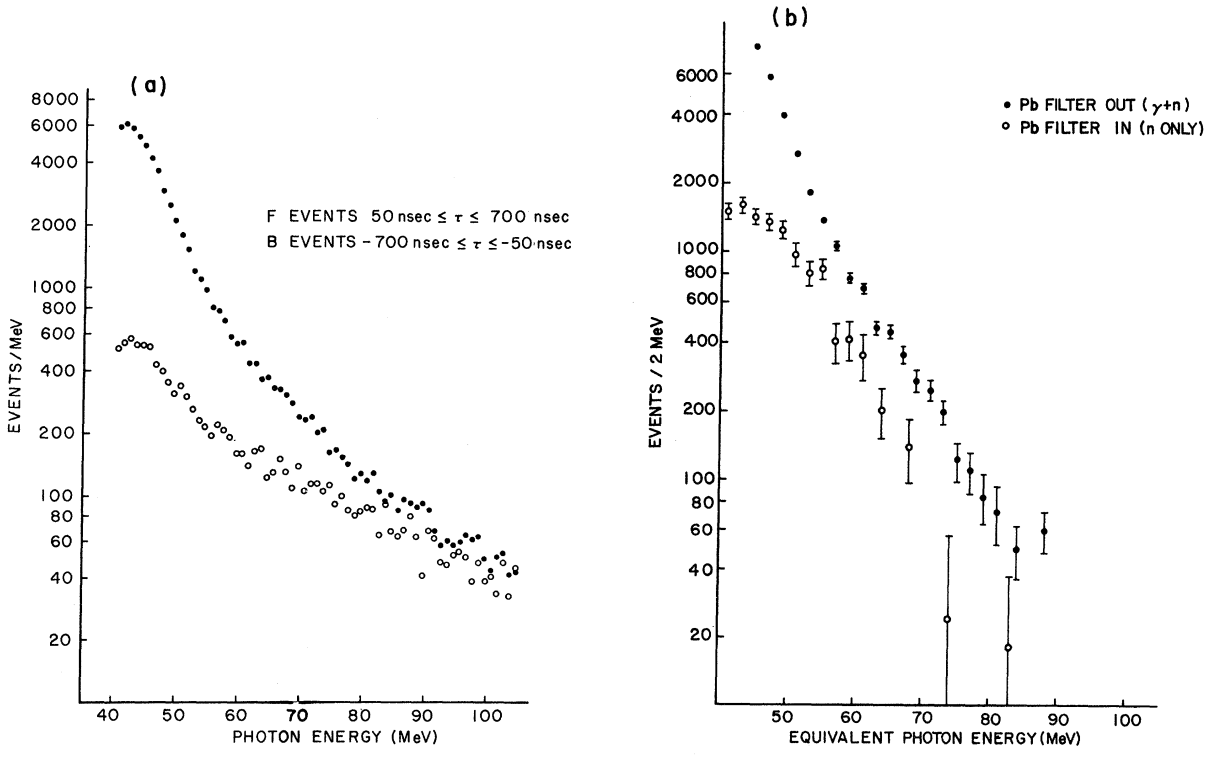

FIG. 2. (a) Energy spectra of B and F events taken with no lead plug. (b) Energy spectra, with and without the lead plug inserted, after background subtraction.

these carbon-bound muons were the source of only 7% of the electron signals. Since nuclear capture by carbon atoms is ~60 times less probable than by calcium, this was thus a negligible source of photons. Finally, the possibility of high-energy neutrons being emitted by the nuclei resulting from muon capture had to be considered. This was checked by conducting separate runs of the experiment with a 5-cm-thick lead slab plugging the collimator in front of the crystal face. This arrangement allowed most neutrons to be detected while 99% of the photons were absorbed by the lead. The very interesting results of this test, namely that neutrons were indeed a large contaminant of our data coming from runs with no lead plug, will be discussed below.

We ran the main part of our experiment for 750 h divided into 85 separate runs, during which time we recorded 4500 neutral events above background between 57 and 90 MeV and within a time gate of 50 to 700 nsec. We also ran for 163 h with the lead plug inserted in the collimator in front of the NaI crystal. In that time, we recorded 310 events above background in the same time and energy intervals.

Figure 2(b) shows the spectra of events taken with and without the lead plug, normalized to the same number of μ stops, after the background has been subtracted. Note the label "Equivalent Photon Energy" since the crystal was calibrated only for photons. Also, it is quite interesting that with the lead plug inserted, events were recorded with equivalent energies of over 80 MeV. Essentially, our reasons for believing that these events (recorded with lead blocking the collimator) were all due to neutrons emitted by nuclei which were excited by muon capture are as follows: First, they were neutral upon entering the lead plug and neutral after leaving it. Second, their foreground time spectrum ($\tau = 387^{+117}_{-175}$ nsec) was consistent with the observed lifetime of muons in calcium. Lastly, since these signals occur at nearly half the rate of neutral events with no lead plug, it is difficult to imagine any process which would create them in the lead from high-energy capture γ rays with such a high efficiency. Also, the energy spectrum of these neutrons may be fitted by an exponential curve with a decay constant of 7 MeV, consistent with that found previously by Sundelin *et al.*[4] below 50 MeV.

To find the fraction of neutrons in the neutral events recorded during our main runs, the efficiency of the lead plug for removing neutrons had to be known. This was determined by a Monte Carlo program to be $(28.0 \pm 0.5)\%$, implying a neutron contamination of $(45 \pm 5)\%$ in our neutral data, where the quoted error is statistical only.

After subtracting out these neutrons we were left with the muon capture-γ-ray spectrum in units of photons per MeV. The rate of radiative capture relative to the total capture rate, $R(E)$, was then derived from the formula

$$n_\gamma(E) = N_\mu f_c R(E) P_T \epsilon(E) V,$$

where $n_\gamma(E)$ is the measured number of photons per MeV.

f_c, the probability that a bound muon was captured by the calcium nucleus, was found to be $(84.9 \pm 0.3)\%$ from the bound-muon lifetime[1] and decay rate.[5] P_T was the probability that a radiated photon fell within our time gate of 50 to 700 nsec and was equal to 74%. The photon detection efficiency, $\epsilon(E)$, was computed from a Monte Carlo program to have the constant value $(2.84 \pm 0.01)\%$ within our energy range. This number was verified experimentally in our runs with the LiH target. $V = 90\%$ was a correction for γ rays which were accidentally vetoed. The number of μ stops, N_μ, could not be taken directly from our scalars since the latter readings would be expected to include some number of π stops, due to pions contaminating the beam.

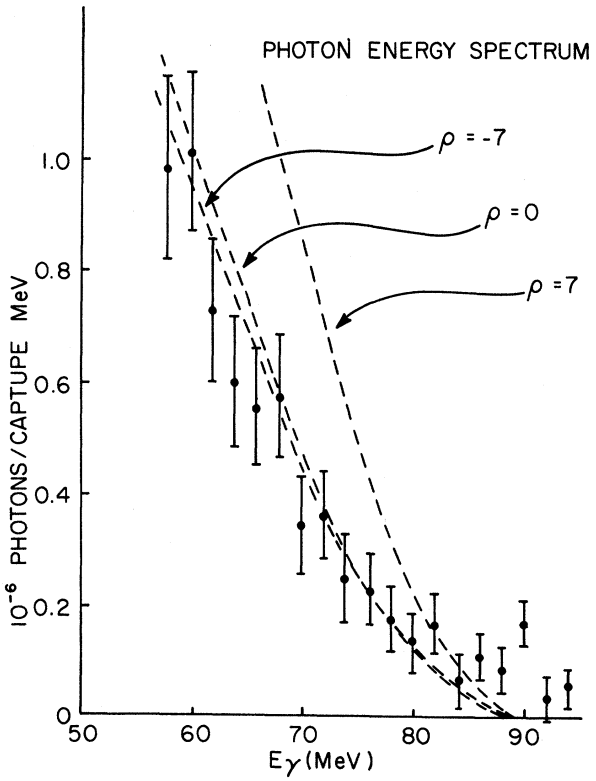

FIG. 3. Relative rate of radiative to normal muon capture. The dashed lines are the relative rates predicted by Rood and Tolhoek for $\rho = -7$, 0, and 7.

Instead, N_μ was calculated from the measured electron time spectrum by the formula

$$n_e = N_\mu f_d P_T \epsilon_e ,$$

where n_e is the total number of electrons detected during the experiment within our time gate; f_d is the probability of a bound muon decaying, 15.1%; and ϵ_e is the efficiency for electron detection, 1.6%. The result was that $N_\mu = (12\,345 \pm 38) \times 10^6$.

The resulting spectrum of $R(E)$ in photons/capture MeV is shown in Fig. 3, where the error bars represent the statistical errors of counting only. The data points are listed in Table I.

We compared the predictions of two theories for radiative muon capture in calcium to our data. The first, by Rood and Tolhoek,[6] assumes an independent particle model for the ^{40}Ca nucleus and applies the closure approximation to a shell model with harmonic-oscillator wave functions. The authors consider radiation by the magnetic moments of the nucleons as well as by the muon and proton charges and include terms proportional to the nucleon momenta. They show that the ratio of radiative to normal muon capture rates is only weakly dependent on nuclear model but rather sensitive to the induced pseudoscalar coupling constant of the weak interaction, g_P, in the region of the value predicted by Goldberger and Treiman,[7] which is +7 times the axial vector coupling constant, g_A. Therefore, by making a least-squares fit of the theoretical photon energy spectrum, with g_P variable, to our experimental data, we should be able to estimate our own value for the induced pseudoscalar.

The other theory we compare to our data is by Fearing[8] and is a direct extension of an earlier work by Foldy and Walecka.[9] The authors include the effects of the giant dipole resonance (GDR) in calcium by relating the dipole part of the nuclear matrix element to an integral over the empirically known photoabsorption cross section, using isospin invariance and Wigner supermultiplet theory. The other multipoles are taken from Rood and Tolhoek.[6] As a result, the absolute rates of radiative and ordinary capture are each lowered by about 35% from that predicted by the shell-model theory[6,10] so their ratio remains the same.[11]

The theoretical spectra for the relative rate[6,8] have as parameters the weak-interaction coupling constants; the maximum photon energy averaged over all states of the final nucleus, E_{max}; and the average neutrino energy in the nonradiative capture, ν. In curve fitting, we generally varied one coupling constant and E_{max}. Since ν was not accurately known, in some cases it was set equal to E_{max} and the two were varied together. Among the coupling constants, emphasis was placed on finding the sign and magnitude of the induced pseudoscalar, which was written as

$$g_P = \left(\rho \frac{m_\pi^2 - m_\mu^2}{m_\pi^2 - q^2} + \delta\right) g_A .$$

The first term expresses the dependence of g_P on the square of the four-momentum transfer, q, and δ represents a possible correction to the one-pion-exchange assumption used in deriving ρ. We therefore expect $\rho \approx +7$ and $\delta \approx 0$.

The resolution function, $f(X)$ (see Table II), was folded into the theoretical energy distribution, $R(E_0)$, according to the formula

$$R'(E) = \int_0^\infty R(E_0) f\left(\frac{E}{E_0}\right) \frac{1}{E_0} dE_0 ,$$

and the resultant photon spectrum, $R'(E)$, was then fitted to the data points of Fig. 3 (Table I). The results from fitting the shell-model theoretical spectrum[6] are shown in Table III. In some cases, the solutions from fitting the GDR model[8] are given in parentheses, but always the two theories gave virtually the same values for the coupling constants. Note that the induced scalar and tensor coupling constants, g_S and g_T, were fitted but gave poor solutions.[12] In varying δ, we found good fits with δ below -12 and E_{max} above 88.6 MeV. We also tried fixing ρ at +7 and varied only E_{max} but could not achieve a good fit. The branching ratio, B, of radiative to normal muon capture in calcium was calculated by integrating the fitted theoretical spectrum, $R(E)$, from 0 MeV to E_{max}.

TABLE I. Photon energy spectrum.

Data points	
E (MeV)	$10^6 R(E)$
58	0.98 ± 0.17
60	1.01 ± 0.15
62	0.73 ± 0.13
64	0.60 ± 0.12
66	0.55 ± 0.11
68	0.57 ± 0.10
70	0.34 ± 0.09
72	0.36 ± 0.08
74	0.24 ± 0.08
76	0.23 ± 0.07
78	0.17 ± 0.06
80	0.13 ± 0.06
82	0.17 ± 0.05
84	0.062 ± 0.051
86	0.10 ± 0.046
88	0.080 ± 0.049
90	0.16 ± 0.044
92	0.029 ± 0.042
94	0.045 ± 0.039

It should be stressed that the shape of this spectrum was set theoretically and that only the high-energy tail was actually within the region of our data. In addition, we may compare the theoretical values of the total muon capture rate, Λ_0 (shown in Table III), as found by substituting the fitted constants into the appropriate theories[9,10] with our measured value[1] of

$$(25.26 \pm 0.21) \times 10^5 \text{ sec}^{-1}.$$

Finally, to determine the effect of choosing $\nu = 90.4$ MeV, one fit was performed with $\nu = 85$ MeV and ρ and E_{max} variable. We see that the lowering of ν was compensated by a similar lowering of E_{max} with ρ remaining unchanged.

An unfortunate complication in interpreting these results is that the theoretical curves which were fitted to our data exhibited a strong mathematical correlation between the induced pseudoscalar coupling constant and maximum photon energy. This is illustrated in Fig. 4, where the curves represent contours of constant probability (i.e., χ^2) about the best fit, which is the point at the center. The relative likelihood is 39% that the true values of ρ and E_{max} fall within the inner contour. The probability for the outer contour is 99%. Furthermore, in the region of our solution, the theoretical function $R(E)$ is rather insensitive to g_p. Keeping all other parameters fixed, Fig. 3 shows the small effect on $R(E)$ as ρ is changed from -7 to 0.

TABLE II. Data points for the energy-resolution function (normalized to unit area).

$X = E_{\text{measured}}/E_{\text{true}}$	$f(X)$
0.712	0.0
0.759	0.429
0.791	0.857
0.823	1.428
0.854	2.070
0.886	2.819
0.918	3.783
0.949	4.854
0.965	5.353
0.981	5.781
0.992	5.839
1.000	5.853
1.009	5.781
1.016	5.710
1.025	5.139
1.041	3.712
1.063	1.285
1.073	0.678
1.079	0.357
1.095	0.0

TABLE III. Results of fitting the shell-model theoretical energy spectrum to our data above 57 MeV. The results for the GDR model are shown in parentheses. Λ_R is the absolute radiative muon capture rate. g_V^β is the vector coupling constant.

Variables	χ^2/degrees of freedom	ρ	δ	g_S/g_V^β	g_T/g_V^β	E_{max} (MeV)	ν	Λ_0 (10^{-5}sec^{-1})	Λ_R (sec^{-1})	$10^4 B$
ρ, E_{max}	12.0(11.1)/14	−5.9(−5.4)	0	0	0	89.4(89.6)	90.4	68.4(45.2)	779.(512)	1.14(1.13)
E_{max}	25.9(22.5)/15	7	0	0	0	83.8(80.7)	90.4	49.9(33.3)	669.(422)	1.34(1.27)
δ, E_{max}	<12.6 /14	7	<−12	0	0	>88.6	90.4	64.6	737.	1.14
$g_S/g_V^\beta, E_{max}$	11.0 /14	7	0	5.0	0	90.57	90.4	331.	3167.	0.96
$g_T/g_V^\beta, E_{max}$	21.4 /14	7	0	0	−24.6	85.7	90.4	78.7	1102.	1.40
ρ, E_{max}	16.1(14.3)/14	−5.9(−5.8)	0	0	0	87.5(87.0)	85.0	55.1(37.7)	693.(460)	1.26(1.22)
						$E_{max} = \nu$				
ρ, E_{max} $(= \nu)$	12.8(11.8)/14	−5.3(−5.2)	0	0	0	89.25(89.6)		63.9(43.7)	763.(511)	1.19(1.17)
E_{max} $(= \nu)$	41.4(77.) /15	7	0	0	0	81.04(76.5)		34.1(20.9)	559.(370)	1.64(1.77)

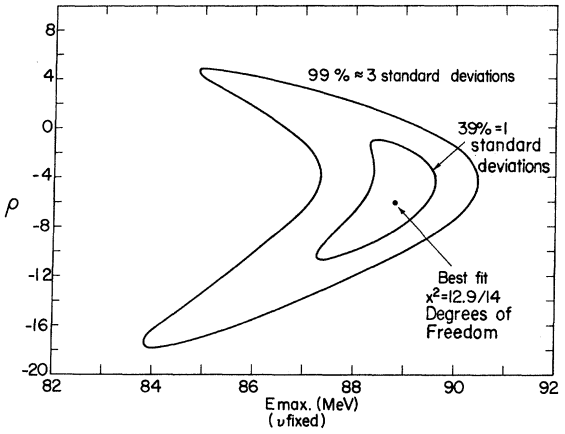

FIG. 4. Contours of constant likelihood (χ^2) in the ρ-E_{max} plane with $\nu = 90.4$ MeV.

Finally, we point out that a much higher rate for radiative muon capture in calcium was reported by Conversi, Diebold, and DiLella,[13] who used a similar experimental setup. However, they did not check for contaminating neutrons and consequently it seems that their spectrum is probably high by roughly 45%. Applying this correction then brings their results into approximate agreement with ours.

In conclusion, Table III shows three sets of fitted parameters having satisfactory χ^2's. The solution with g_S variable we discount because of its associated huge value for Λ_0. The solution with δ variable meets all requirements but we feel that this is probably due to the close theoretical relationship between δ and ρ, as given in our expression for g_P. We are then left with the fit with ρ and E_{max} variable as fundamentally our best solution.

Although this value of ρ ($= -5.9$) is in sharp disagreement with the Goldberger-Treiman prediction of $\rho = +7$, it must be remembered that many approximations were made in deriving the theoretical formulas we used and that these should certainly be reviewed[14] before any final conclusions are made on the significance of our result for ρ.

The authors wish to thank Dr. L. DiLella for extensive work in the design and running of this experiment and for many helpful comments during its analysis.

---

*Research supported in part by the National Science Foundation.

†Present address: Department of Physics and Astronomy, Tel-Aviv University, Tel-Aviv, Israel.

[1]L. DiLella, I. Hammerman, and L. M. Rosenstein, Phys. Rev. Lett. 27, 830 (1971).

[2]L. G. Pondrom and A. Strelzoff, Rev. Sci. Instrum. 34, 362 (1963).

[3]For a more detailed account of our method for measuring energy and time delays see L. M. Rosenstein, Columbia University, Nevis Report No. 191, 1972 (unpublished).

[4]R. M. Sundelin *et al.*, Phys. Rev. Lett. 20, 1198 (1968).

[5]R. W. Huff, Ann. Phys. (N.Y.) 16, 288 (1961).

[6]H. P. C. Rood and H. A. Tolhoek, Nucl. Phys. 70, 658 (1965).

[7]M. L. Goldberger and S. B. Treiman, Phys. Rev. 111, 354 (1958).

[8]H. W. Fearing, Phys. Rev. 146, 723 (1966).

[9]L. L. Foldy and J. D. Walecka, Nuovo Cimento 34, 1026 (1964).

[10]J. R. Luyten, H. P. C. Rood, and H. A. Tolhoek, Nucl. Phys. 41, 236 (1963).

[11]Actually, because of a computational error, Fearing concluded that the ratio would increase.

[12]Although the curve fitted with g_S variable had a low χ^2 of 11, the absolute capture rates Λ_0 and Λ_R were extremely high and we therefore rejected this solution.

[13]M. Conversi, R. Diebold, and L. DiLella, Phys. Rev. 136, B1077 (1964).

[14]H. P. C. Rood and A. F. Yano, Phys. Lett. 35B, 59 (1971). A. F. Yano, F. B. Yano, and H. P. C. Rood, Phys. Lett. 37B, 189 (1971).